Academic Sciences International Journal of Pharmacy and Pharmaceutical Sciences

ISSN- 0975-1491 Vol 3, Issue 4, 2011

Research Article

3D-QSAR AND DOCKING STUDIES OF FLAVONOID DERIVATIVES ON p56^{lck} PROTEIN TYROSINE KINASE USING PLS

ROHITH KUMAR A*, SRI RAMYA. TATA, SHRAVAN KUMAR. GUNDA

Bioinformatics Division, PGRRCDE, Osmania University, Hyderabad 500007, Andhra Pradesh, India. *Email: rohit.casper@gmail.com

Received: 19 Apr 2011, Revised and Accepted: 7 Jul 2011

ABSTRACT

3D-QSAR studies of p56^{lck} protein tyrosine kinase inhibitory activity of 50 Flavonoid derivatives were performed by comparative molecular field analysis (CoMFA) and comparative molecular similarity indices (CoMSIA) methods to rationalize the structural requirements responsible for the inhibitory activity of these compounds. The best predictions for the protein tyrosine kinase were obtained with the CoMFA standard model (q^2=0.859, r^2=0.972) and CoMSIA model combined steric, electrostatic and hydrophobic fields (q^2=0.673, r^2=0.961). The contour maps from 3D-QSAR models in combination with docked binding structures help to better interpret the structure activity relationship and also to position the inhibitors into the p56^{lck} active site taken from the X-ray crystal structures of the Human p56^{lck} tyrosine Kinase SH2 Domain (PDB code 1LKK).

Keywords: Flavonoids, 3D-QSAR, CoMFA, CoMSIA, Molecular Docking, PTKs (Protein Tyrosine Kinases)

INTRODUCTION

Drug–target interaction is a process of molecular recognition. Target molecules can be molecules from either a pathogen or its host; they are typically enzymes but may include proteins such as receptors or regulatory factors and thus proteins are implicated as potential drug targets, their identification and structural analysis are of prime importance in rational drug design. When drugs associate with a target molecule, the drug evokes the desired biological effect either by inhibiting or activating the target molecule and this interaction occurs in specific conformation. It is clear that for understanding this interaction the knowledge of the 3D structure is of crucial importance. The most reliable data on 3D structures are obtained by X–ray diffraction or by multi–dimensional NMR measurements. Unfortunately, these kind of experimental data are rather scarce. Therefore, computational modeling techniques play an important role in drug research. The fusion of combinatorial chemistry and high-throughput screening technology is dramatically shortening the time needed to discover new compounds and develop drugs candidates. These technologies rely on advanced automation, miniaturization, and computational components[1].

In the present study, we considered inhibitory effect of flavonoids on protein tyrosine kinases (PTKs) which provide a central switching mechanism in cellular signal transduction pathways by catalyzing the transfer of the γ-phosphate of either ATP or GTP to specific tyrosine residues in certain protein substrates[2]. This regulatory control plays a crucial role in signal transduction pathways that regulate several cellular functions under both normal and deregulated conditions[3]. PTKs are the intracellular effectors for many growth hormone receptors. After the discovery of activated PTKs as the product of dominant viral transforming genes (oncogenes) enough evidence are now available to suggest that inappropriate or elevated expression of PTKs contribute to the transformed state of cells in many human malignancies. P56^{lck} is a lymphoid-specific protein tyrosine kinase that is principally expressed in T lymphocytes[4]. Association of p56^{lck} with the cytoplasmic tail of various cell surface receptors, as well as associations of p56^{lck} with intracellular targets of phosphorylation, suggests that this tyrosine kinase plays a central role in coordinating early signal transduction events[5]. The key step in the mechanism of kinase activity of all PTKs is the recognition and binding of a nucleoside triphosphate (usually ATP) and an appropriate tyrosyl-containing substrate to the enzyme. Direct transfer of phosphate between the two molecules is the next step in the PTKs function.

A variety of compounds can inhibit the function of PTKs in a manner which is competitive with respect to nucleotide binding[6]. Among such competitive inhibitors are flavonoids, a group of polyphenolic compounds occurring in plants, where they play a role in many physiological process[7]. They are classified according to the saturation level and opening of the central pyran ring, mainly into flavonols, flavones, flavanols (cathechins), flavanones, isoflavones and anthocyanins. This group of plant pigments is largely responsible for the colors of many fruits and flowers. The word flavonoids comes from the Latin flavus which means yellow; however some flavonoids are red, blue, purple, or white. They were discovered, along with vitamin C, in 1928 by Albert Szent-Gyorgyi, who called them vitamin P[8, 9]. Chemically they are C6 -C3 -C6 compounds in which the two C6 groups are substituted benzene rings, and the C3 is an aliphatic chain which contains a pyran ring. Flavonoids occur as O- or C-glycosides or in the Free State as aglycones with hydroxyl or methoxyl groups present on the aglycone[10]. The flavonoids may be divided into seven types: flavones, flavonols, flavonones, chalcones, xanthones, isoflavones, and biflavones. Some of the best food sources of flavonoids are red wine, apples, blueberries, bilberries, onions, soy products and tea. The average daily intake of flavonoids in the United States is between 150 and 200 mcg. Numerous medicinal plants contain therapeutic amounts of flavonoids, which are used to treat disorders of the peripheral circulation, to lower blood pressure, to improve aquaresis and as anti-inflammatory, antispasmodic and anti-allergic agents[11]. The many pharmacological effects of flavonoids are linked to their ability to act as strong antioxidants and free-radical scavengers, to chelate metals, and to interact with enzymes, adenosine receptors, and biomembranes. Some flavonoids also possess antimicrobial activity[12].

Several QSAR studies were reported on inhibitory activity of flavonoids against protein–tyrosine kinase p56^{lck} using different descriptors and different methods of modeling. Among various methods of QSAR[13], we considered two strategies comparative molecular field analysis (CoMFA) and comparative molecular similarity indices analysis (CoMSIA) and the relation between the descriptors in each strategy is obtained by PLS method by using the CoMFA/CoMSIA descriptors as independent variables and pIC_{50} values as a dependent variable in PLS regression analysis and CoMFA and CoMSIA coefficient maps were generated and non-validated r^2 is obtained from the maps.

MATERIALS AND METHODS

Data set

In the present study, the in vitro inhibitory activity data (IC_{50}) of the 50 Flavonoid derivates on p56^{lck} protein was taken from the literature[14]. The structures of the compounds and their biological data are given in Table 1. The IC_{50} values were converted to the

corresponding pIC_{50} ($-logIC_{50}$) and used as dependent variables in CoMFA and CoMSIA analysis. The pIC_{50} values span a range of 3-log units providing a broad and homogenous data set for 3D-QSAR study. The 3D-QSAR models were generated using a training set of 36 molecules. Predictive power of the resulting models was evaluated using a test set of 14 molecules. The test set compounds were selected randomly such that a wide range of activity in the data set was included.

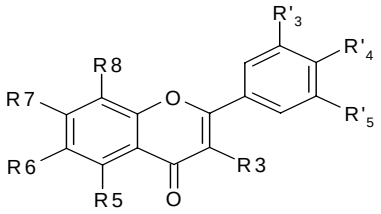

Table 1: The 50 compounds are shown in the table which is based on this core scaffold

Compound	R_3	R_5	R_6	R_7	R_8	R'_3	R'_4	R'_5
1	H	OH	H	OH	H	H	NH_2	H
2	OH	OH	H	OH	H	OH	OH	H
3	OH	H	H	OH	H	OH	OH	H
4	H	OH	H	OH	H	H	OH	H
5	H	OH	H	H	H	H	OH	H
6	H	H	OH	H	H	OH	H	H
7	H	NH_2	OH	NH_2	H	H	NH_2	H
8	H	OH	H	OH	H	H	H	H
9	H	H	H	H	H	OCH_3	OH	OCH_3
10	H	OH	H	OH	H	OH	OH	H
11	H	H	H	OH	H	OH	H	H
12	H	NH_2	OH	NH_2	H	NH_2	H	H
13	H	H	OMe	H	NH_2	NH_2	H	H
14	H	H	OH	H	H	OCH_3	OCH_3	OCH_3
15	OH	OH	H	OH	H	OCH_3	OH	OCH_3
16	OH	OH	H	OH	H	OH	H	OH
17	H	H	NH_2	H	H	H	NH_2	H
18	H	H	NH_2	H	NH_2	H	NH_2	H
19	H	H	OH	H	NH_2	H	NH_2	H
20	H	H	OH	H	H	H	OH	H
21	H	H	H	OH	OH	OCH_3	OH	OCH_3
22	H	H	H	H	NH_2	H	NH_2	H
23	H	H	OH	H	H	OCH_3	OH	OCH_3
24	H	H	H	OH	H	H	NH_2	H
25	H	H	NH_2	OH	H	H	NH_2	H
26	H	H	H	OH	H	H	OH	H
27	H	H	H	OH	OH	OH	H	H
28	H	H	NH_2	H	H	NH_2	H	H
29	H	H	H	H	H	H	NH_2	H
30	H	OH	NH_2	H	H	H	NH_2	H
31	OH	OH	H	OH	H	H	H	H
32	H	OH	H	OCH_3	H	H	OH	H
33	H	OH	H	H	H	OH	H	H
34	H	H	H	OH	OH	H	H	H
35	H	OH	H	H	NH_2	H	NH_2	H
36	H	H	H	OH	NH_2	H	NH_2	H
37	H	H	H	OH	H	H	H	H
38	H	H	OCH_3	H	NH_2	H	NH_2	H
39	H	H	H	OH	OH	OCH_3	OCH_3	OCH_3
40	$COOCH_3$	H	H	H	H	H	OH	H
41	H	H	H	H	H	H	OH	H
42	H	H	NH_2	OH	H	NH_2	H	H
43	H	H	NH_2	OH	NH_2	H	NH_2	H
44	$COOCH_3$	H	H	H	H	H	NH_2	H
45	COOH	H	H	OCH_3	H	H	OH	H
46	H	H	H	OH	H	OCH_3	OH	OCH_3
47	H	H	NO_2	OH	NO_2	H	NO_2	H
48	COOH	H	H	H	H	H	OH	H
49	H	OCH_3	H	H	NH_2	H	NH_2	H
50	H	H	H	OH	NO_2	H	NO_2	H

Alignment

Molecular conformation and orientation is one of the most sensitive input areas in 3D-QSAR studies. One of the steps in CoMFA and CoMSIA methods is the determination of active conformation and alignment of molecules. The success of CoMFA and CoMSIA methods entirely depend on the relative positioning of the ligands in the fixed lattice, prior to the generation of 3-D descriptors. In the present study, superimposition of the molecules was carried out by using compound 50 as template structure.

These alignments were subsequently used in CoMFA/CoMSIA probe interaction energy calculations and FlexX method to derive docked conformations.

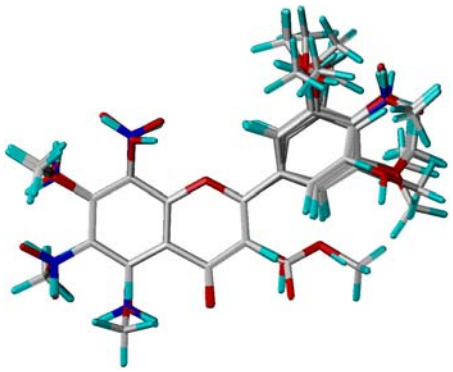

Fig. 1: Structure alignment of the compounds in the training set and test set

Molecular docking

Docking is a method which predicts the preferred orientation of one molecule to a second when bound to each other to form a stable complex. Knowledge of the preferred orientation in turn may be used to predict the strength of association or binding affinity between two molecules using for example scoring functions.

Docking studies were carried out using the FlexX program[15] interfaced with SYBYL 6.7. In this automated docking program, the flexibility of the ligands is considered while the protein or biomolecule is considered as a rigid structure. The ligand is built in an incremental fashion, where each new fragment is added in all possible positions and conformations to a pre-placed base fragment inside the active site. All the molecules for docking were sketched in the SYBYL and minimized using Gasteiger-Hückel method and all the charges were removed. The 3D coordinates of the active sites were taken from the X-ray crystal structure of the Human p56^{lck} tyrosine kinase SH2 Domain in complex with the phosphotyrosyl peptide AC-PTYR-GLU-GLU-ILE (PYEEI PEPTIDE) (PDB code 1LKK) reported as complex with the corresponding agonist having an resolution of 1.00 Å. Formal charges were assigned to all the molecules and FlexX run was submitted.

CoMFA and CoMSIA studies

For the CoMFA[16] calculations, steric and electrostatic field energies were calculated using sp^3 carbon as the steric probe atom and a +1 net charge as the electrostatic probe. The cutoff was set to 30kcal/mol. The minimum σ (column filtering) was set to 2.0kcal/mol to improve the signal-to-noise ratio by omitting those lattice points whose energy variation was below this threshold. Regression analysis was performed using the cross validation of compounds leave-one-out method[17]. CoMSIA[18] calculates similarity indices at the intersections of a surrounding lattice. The charge, probe, and grid spacing used to construct the CoMFA best model were also used for the CoMSIA investigation. Five physicochemical properties of steric, electrostatic, hydrophobic, hydrogen bond donor, and hydrogen bond acceptor fields were calculated. The lattice dimensions were selected with a sufficiently large margin (4Å) to enclose all aligned molecules. The statistical evaluation for the CoMSIA analysis was carried out in the same way as described in CoMFA.

Table 2: Experimental pIC_{50}, predicted pIC_{50} and residual values of molecules in the training set for CoMFA and CoMSIA

Compound	Observed Activity pIC_{50}	Predicted Activity (CoMFA)	Residual	Predicted Activity (CoMSIA)	Residual
1	5.13	4.844	0.286	4.567	0.563
10	4.46	4.334	0.126	4.457	0.003
11	4.41	4.528	-0.118	4.372	0.038
12	4.34	4.385	-0.045	4.393	-0.053
14	4.22	3.902	0.318	3.578	0.642
15	4.16	4.657	-0.497	4.753	-0.593
17	3.99	3.888	0.102	3.752	0.238
18	3.97	4.051	-0.081	3.763	0.207
19	3.93	3.962	-0.032	4.246	-0.316
2	4.88	4.955	-0.075	5.145	-0.265
20	3.93	3.596	0.334	3.888	0.042
22	3.91	3.667	0.243	3.632	0.278
23	3.89	3.997	-0.107	3.985	-0.095
25	3.85	3.762	0.088	3.796	0.054
27	3.75	3.547	0.203	3.911	-0.161
28	3.70	3.541	0.159	3.302	0.298
29	3.68	3.687	-0.007	3.768	-0.088
3	4.86	4.82	0.04	4.526	0.334
30	3.65	4.141	-0.491	4.168	-0.518
32	3.55	3.688	-0.138	3.661	-0.111
33	3.50	3.517	-0.017	3.647	-0.147
34	3.50	3.479	0.021	3.787	-0.287
35	3.49	3.332	0.158	3.582	-0.092
37	3.47	3.348	0.122	3.497	-0.027
39	4.40	3.452	-0.052	3.88	-0.48
4	4.83	4.459	0.371	4.417	0.413
41	3.30	3.722	-0.422	3.706	-0.406
42	3.30	3.571	-0.271	3.656	-0.356
44	3.09	2.963	0.127	3.21	-0.12
45	2.99	2.843	0.147	2.707	0.283
46	2.90	3.212	-0.312	3.444	-0.544
47	2.81	2.603	0.207	3.736	-0.092
48	2.80	3.127	-0.327	3.08	-0.28
50	2.73	3.299	-0.569	2.099	0.631
7	4.74	4.625	0.115	4.659	0.081
8	4.71	4.681	0.029	4.255	0.455

Partial least square (PLS) analysis

PLS method[19] was used to linearly correlate the CoMFA and CoMSIA fields to biological activity values. The cross-validation was performed using leave-one-out (LOO) method in which one compound is removed from the dataset and its activity is predicted using the model derived from the rest of the molecules in the dataset. Equal weights for CoMFA were assigned to steric and electrostatic fields using CoMFA STD scaling option. To speed up the analysis and reduce noise, minimum column filter value of 2.0kcal/mol was used for the cross-validation. Non-cross-validation was performed to calculate conventional r^2 using the same number of components. To further assess the robustness and statistical confidence of the derived models, bootstrapping analysis for 100 runs was performed[20]. Bootstrapping involves the generation of many new data sets from original data set and is obtained by randomly choosing samples from the original data set. The statistical calculation is performed on each of these bootstrapping samplings. The difference between the parameters calculated from the original data set and the average of the parameters calculated from the many bootstrapping samplings is a measure of the bias of the original calculations. The entire cross-validated results were analyzed considering the fact that a value of q^2 above 0.3 indicates that probability of chance correlation is less than 5% [21].

RESULTS AND DISCUSSIONS

CoMFA and CoMSIA analysis

Comparative molecular field analysis and Comparative molecular similarity indices analysis are 3D-QSAR methods intended to correlate the molecular features of a series of compounds with biological activities. CoMFA is based on the calculation of steric and electrostatic fields, while CoMSIA also considers hydrophobic, hydrogen bond acceptor and hydrogen bond donor fields. CoMFA and CoMSIA may be extremely sensitive to molecular alignment rules and overall consistency of the molecular alignment, therefore, the determination of spatial molecular alignment is a crucial step in 3D-QSAR studies, since the analysis are highly dependent on the quality of the alignments. The molecular docking studies were carried out using the program FlexX in order to generate receptor based alignment for model building. The advantage of a docking-based model is that we can directly superimpose the contour maps into the protein active site. Such superimposition will also allow us to check the correlation between the contour maps and the corresponding receptor residues present near them. We used X-ray crystal structures of the Human $p56^{lck}$ tyrosine kinase SH2 Domain in complex with the phosphotyrosyl peptide AC-PTYR-GLU-GLU-ILE (PYEEI PEPTIDE) (PDB code 1LKK) for molecular studies.

Table 3: Experimental pIC_{50}, predicted pIC_{50} and residual values of molecules in the test set for CoMFA and CoMSIA

Compound	Observed Activity pIC_{50}	Predicted Activity (CoMFA)	Residual	Predicted Activity (CoMSIA)	Residual
13	4.25	4.64	-0.39	4.52	-0.27
16	4.00	4.47	-0.47	4.43	-0.43
21	3.92	4.36	-0.44	4.25	-0.33
24	3.86	3.57	0.29	3.49	0.37
26	3.78	3.61	0.17	4.18	-0.4
31	3.53	3.66	-0.13	3.42	0.11
36	3.48	3.29	0.19	3.41	0.07
38	3.43	3.09	0.34	2.95	0.48
40	3.36	3.21	0.15	3.91	-0.55
43	3.12	3.57	-0.45	3.59	-0.47
49	2.79	2.65	0.14	3.08	-0.29
5	4.80	4.23	0.57	4.09	0.71
6	4.80	4.45	0.35	4.64	0.16
9	4.57	4.36	0.21	4.39	0.18

In CoMFA, the steric and electrostatic contributions were found to be 49.3% and 50.7% respectively. Therefore, the electrostatic field had a greater influence than the steric field, indicating that the electrostatic interactions of the molecules with the receptor could be an important factor for $p56^{lck}$ protein tyrosine kinase activity. CoMSIA models with different combinations of steric, electrostatic, hydrophobic, hydrogen bond donor and hydrogen bond acceptor fields were also evaluated by Leave-one-out and test set evaluation. The steric, electrostatic, hydrophobic, hydrogen bond donor and hydrogen bond acceptor contributions were found to be 69.9%, 34.3%, 15.7%, 18.6% and 24.5% respectively. These models showed good correlative and predictive values which indicated that the CoMSIA models were less dependent on the fields employed. Partial least square analysis was carried out for the training set molecules and the results are presented in Table 4 which shows that CoMFA model with LOO q^2 value of 0.859 and CoMSIA model with q^2 value of 0.673 was obtained. The no-validation PLS analysis resulted in conventional r^2 of 0.972, F value of 209.820 and standard error value of 0.116 for CoMFA model and r^2 of 0.961, F value of 119.988 and standard error value of 0.140 for CoMSIA model.

Table 4: Statistical results of CoMFA and CoMSIA models

PLS Statistics	CoMFA	CoMSIA
q^2	0.649	0.714
r^2	0.987	0.998
N	5	6
F value	319.734	1708.976
SEE	0.062	0.025
CV	0.626	0.717
r2bootstrap	0.995	0.999
Sbootstrap	0.043	0.019
Field contributions %		
Steric	65.2	20.8
Electrostatic	34.8	22.6
Hydrophobic	-	15.4
Hydrogen Bond Donor	-	19.4
Hydrogen Bond Acceptor	-	21.4

The observed and calculated (predicted) activity values of training set and test set molecules for CoMFA and CoMSIA are given in Table 2 and Table 3. The plots of observed versus calculated activity values for training set molecules and test set molecules for CoMFA and CoMSIA analysis are shown in Figs 2 and 3.

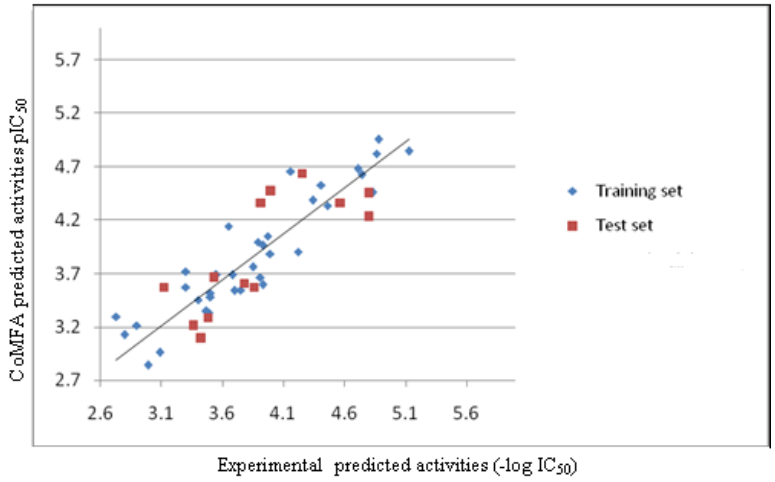

Fig. 2: Predicted activities by CoMFA model versus experimental predicted activities of Flavonoid derivatives. Filled rhombus shapes indicate compounds of training set; Filled squares indicate compounds of the test set

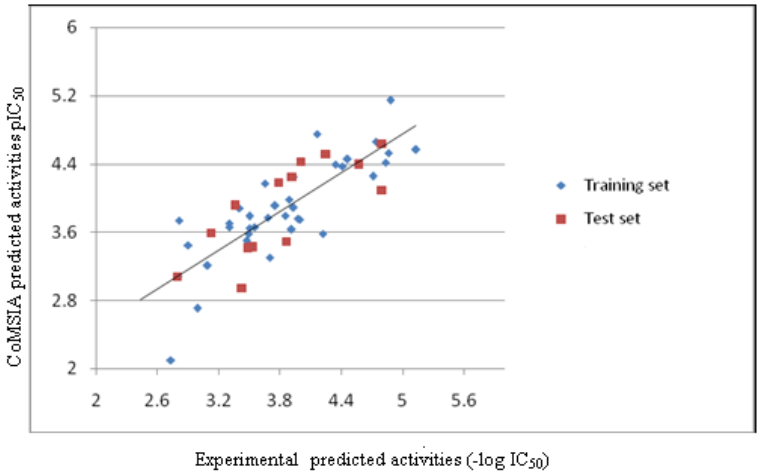

Fig. 3: Predicted activities by CoMSIA model versus experimental predicted activities of Flavonoid derivatives. Filled rhombus shapes indicate compounds of training set; Filled squares indicate compounds of the test set

CoMFA and CoMSIA contour maps

CoMFA and CoMSIA contour maps with a best-fit model were generated. In the figures, the isocontour diagrams of the field contributions for different properties calculated by the CoMFA and CoMSIA analysis are illustrated with exemplary ligands. Selectivity fields depict the change in binding preference occurring upon the change in molecular field around the ligands. Contour plots may help identify important regions where any change may affect binding preference. Furthermore, they may be helpful in identifying important features contributing to interactions between the ligand and the active site of a receptor. For the CoMFA steric, electrostatic fields and CoMSIA steric, electrostatic, hydrophobic, donor and acceptor fields, the contours represent 80% and 20% level contributions. For convenience, all similar contour map positions were labeled and shown in combination with the highly active compound no. 50.

The CoMFA green contours (Fig. 4(a)) indicates the area in which steric bulk might have a positive effect on activity while the yellow region is unfavorable for bulky groups. Green contours are mainly present at R_5 and R_7 side groups, which indicate that substitution with bulky steric groups, increase the activity of the compound. This may be the reason why compounds with OH substituents in this area are having favorable bulky regions than other molecules. The yellow contours present at the R'_4 group of phenyl ring shows that bulky groups are unfavorable. This can be explained by the fact that the compounds with NO_2 substitution in this area, e.g., 47 and 50, are having unfavorable bulky groups.

The CoMFA electrostatic contour plots are displayed in Fig. 4(b). The blue contour indicates the region where positive groups are required for high activity while the red zone indicates a region favorable for negative groups. One blue contour map exist near the ring positioned near the R_6 and R_7 group suggesting that there is a requirement of positive charge group at this position. Three red contours exist in the molecule, positioned above R_7, R_8 side groups and also near R'_4 and R'_5 groups. This can be explained as the compounds with NO_2 substituents, e.g., 47 and 50, have good activity when compared with the other compounds without this substituent.

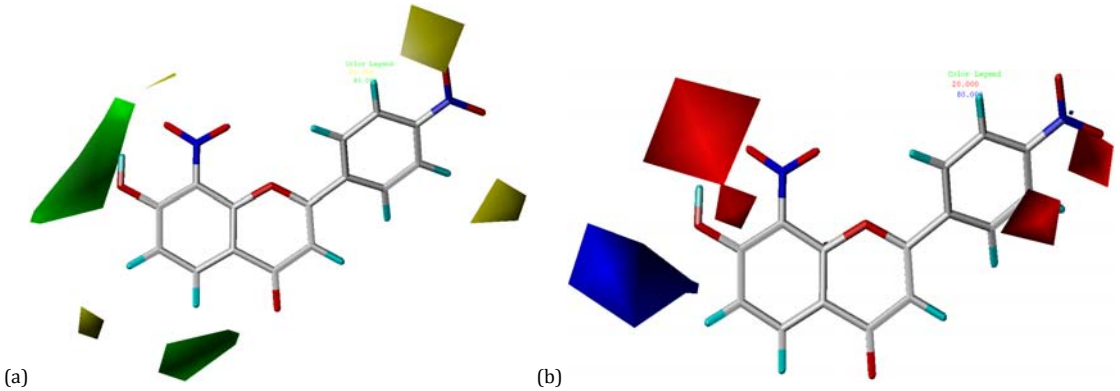

(a) (b)

Fig. 4: CoMFA contour maps are shown in the presence of the most compound 50. (a) Steric fields (b) Electrostatic fields

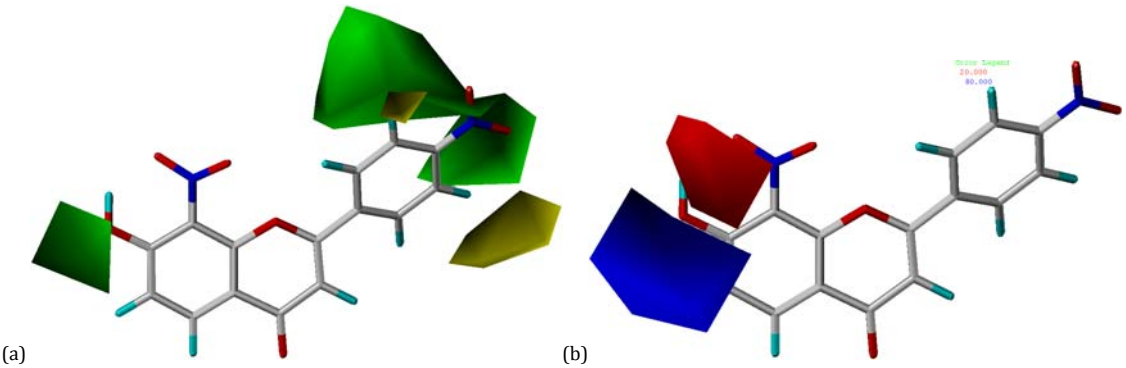

(a) (b)

Fig. 5: CoMSIA contour maps for steric and electrostatic are shown in the presence of the most potent compound 50. (a) Steric fields (b) Electrostatic fields

The CoMSIA contour plots employing steric, electrostatic, hydrophobic, hydrogen donor and hydrogen acceptor are shown in Fig. 5(a) and 5(b). These contours are almost the same as the CoMFA-steric and electrostatic contours (Fig. 4). But in the CoMSIA electrostatic model, two red contours maps are absent at the position R'_4 and R'_5, and there is presence of a large blue contour map at R_6 and R_7 positions.

In Figure 6(a), two white contours were showing unfavorable hydrophobic interaction regions near R_7 and R'_4. This unfavorable region at R'_4 position is due to the NO_2 substituent which is similar to that of the yellow steric contour in Fig. 5(a). Only a small part of yellow contour is present below the phenyl ring of R_6 group, which indicates that any bulk group present at this position will represent hydrophobically favored regions. The Hydrogen-bond donor contour maps in Fig 6(b) signify the regions of hydrogen-bond donor favorable (cyan) and unfavorable (purple) regions. Cyan contours are seen near the R_7, R_8 position, indicating that hydrogen bond donor functionalities in this region will enhance activity. There are large regions of purple contours present on the phenyl ring and also at R_8 and R'_4 positions, indicating an unfavorable regions for hydrogen bond donor groups.

Figure 6(c) shows the CoMSIA hydrogen bond acceptor field, denoted by magenta and red contours. Magenta contours represent regions where hydrogen bond acceptors on compounds are favorable, and red contours indicate regions where hydrogen bond acceptors on inhibitors are unfavorable for the activity. The small red contours represent the three-membered ring, but the large magenta contour present indicates that, in this position, any substituent containing an acceptor group increases the activity. The red regions are mainly present at the R_8 and R'_4 positions, the presence of NO_2 on the phenyl ring is responsible for unfavorable regions on the compound. The large magenta contour located at the R_5, R_6 and R_7 positions in Fig. 6(c) indicate that substituent's with hydrogen-bond acceptors are favored in these areas.

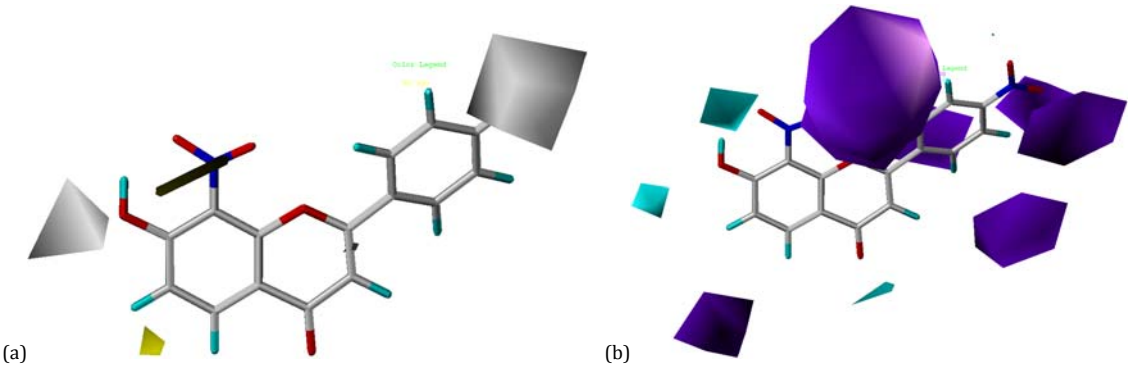

(a) (b)

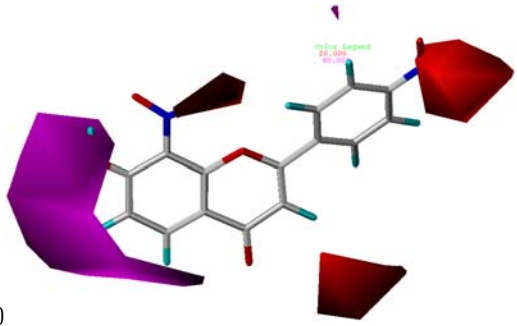

(c)

Fig. 6: CoMSIA contour maps for hydrophobic, hydrogen-bond donor and acceptor are shown in the presence of the most potent compound 50. (a) Hydrophobic fields (b) Hydrogen-bond donor fields (c) Hydrogen-bond acceptor fields

Docking results

The docking experiments were partly carried out with the X-ray crystal structures of the Human p56^{lck} tyrosine kinase SH2 Domain in complex with the phosphotyrosyl peptide AC-PTYR-GLU-GLU-ILE (PYEEI PEPTIDE). All atoms of the protein were treated as aggregates, with the exception of those within the 6.5 Å radius of the bound ligand (Phosphotyrosyl peptide AC-PTYR-GLU-GLU-ILE (pyeei peptide)). The ligand (Phosphotyrosyl peptide AC-PTYR-GLU-GLU-ILE (pyeei peptide)) was pre-processed before docking calculations by giving charges according to the Gasteiger-Hückel method followed by energy minimization with 10,000 iterations of conjugate gradient algorithm using Tripos force field. By using the FlexX module in the SYBYL 6.7 package, Phosphotyrosyl peptide AC-PTYR-GLU-GLU-ILE (pyeei peptide) was docked into both the crystal structure and the relaxed one. For both structures the active sites include all residues within 6.5Å radius of the bound ligand and metals. Other functions were set to default values.

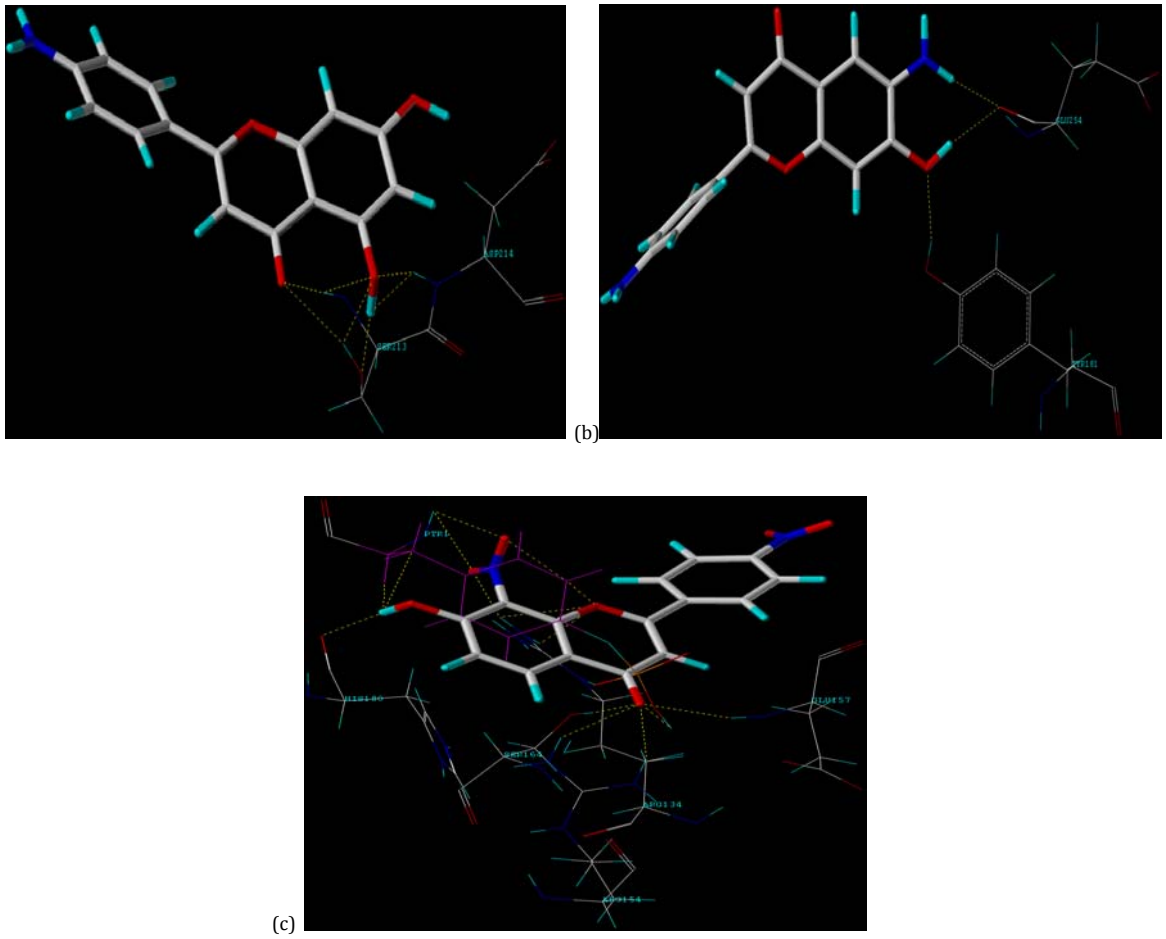

(a) (b)

(c)

Fig. 7: The active site of Crystal structure of Human p56^{lck} tyrosine kinase with important amino acid residues (shown in stick model) and the docked ligand of (a) compound 1, (b) compound 25, (c) most active compound 50, where these compounds are shown in capped stick model

Out of three compounds (Fig 7(a), (b) and (c)) which were docked into receptor site by using FlexX, compound no. 50 showed more interactions with the Human $p56^{lck}$ tyrosine kinase than the other 2 compounds, this is due to the high activity it posses. Along with the residues of the $p56^{lck}$, it also shows interactions with the ligand PTR1. Compound no.50 showed 14 interactions with 4 residues and 1 ligand, while compound no.1 showed 6 interactions with 2 residues and compound no.25 showed just 3 interactions with 2 amino acids. The interactions along with the distance between the compound and ligand are shown in Table 5.

Table 5: Docking results showing the interactions of three compounds

Compound	Amino acid	Interaction	Distance (Å)
1	Ser213	O11-H	1.856
		O11-HG	2.194
		O18-H	2.695
		O18-HG	1.782
		OG-H8	1.736
1	Asp214	O18-H	1.680
25	Tyr181	O18-HH	1.869
25	Glu254	O-H8	1.981
		O-H9	1.796
50	Arg134	O7-HH21	1.968
		O7-HH22	2.730
		O24-HH22	1.807
50	Arg154	O11-HH22	2.674
		O11-HH12	2.011
50	Glu157	O11-H	2.369
50	Ser164	O11-HG	1.934
50	PTR (ligand)	O11-H7	1.150
		O23-H	2.672
		O23-CE2	2.175
		H8-11A	2.024
		H8-CB	2.204
		O7-CE2	1.966
		O24-H	2.262

CONCLUSION

In conclusion, our present studies have established that CoMFA and CoMSIA models are quite reliable to efficiently guide further modification in the molecules for obtaining better drugs. They have provided good statistical results in terms of q^2 and r^2 values for flavonoid derivatives. Both CoMFA and CoMSIA models provided the significant correlations of biological activities with steric and electrostatic fields, establishing the significance of steric and electrostatic fields in the selectivity and activity of the compounds. However, in comparison to CoMSIA the CoMFA method was found to provide a slightly better statistical model. However, the reliability of both the models was verified by the compounds in the testing set. The 3D-QSAR results revealed some important sites, where steric, electrostatic, hydrophobic, hydrogen-bond donor and hydrogen-bond acceptor modifications should significantly affect the bioactivities of the compounds. The 3D contour plots derived from the CoMFA, CoMSIA and docking provided vital clues that can be used to design new molecules with improved kinase inhibitory activity.

ACKNOWLEDGEMENT

We are grateful for the financial support from UGC Govt. of India and also the management of PGRRCDE, Osmania University for providing the software facility and for continuous support to carry out this work.

REFERENCES

1. Hansch C, Leo A. Exploring QSAR. Fundamentals and Applications in Chemistry and Biology, ACS professional reference book, American chemical society, Washington D.C; 1996.
2. Blume-Jensen P, Hunter T. Oncogenic Kinase C Signalling. Nature 2001; 411:355-365.
3. Hunter T. Signaling — 2000 and Beyond. Cell 2000; 100:113-127.
4. Schlessinger J. Cell Signaling by Receptor Tyrosine Kinases. Cell 2000; 103:211-225.
5. Cantley LC, Auger KR, Carpenter C, Duckworth B, Graziani A, Kapeller R, et al. Oncogenes and Signal Transduction. Cell 1991; 64:281-302.
6. Bolen JB, Veillette A, Schwartz AM, DeSeau V, Rosen N. Activation of pp60c-src Protein Kinase Activity in Human Colon Carcinoma. Proc Natl Acad Sci 1987; 84:2251-2255.
7. Slamon DJ, Clark GM, Wong SG, Levin WJ, Ullrich A, McGuire WL. Human Breast Cancer: Correlation of Relapse and Survival with Amplification of the HER-2/neu Oncogene Science 1987; 235:177-182.
8. Anderson SJ, Levin SD, Perlmutter RM. Involvement of the Protein Tyrosine Kinase $p56^{lck}$ in T Cell Signaling and Thymocyte Development. Adv Immuno 1994; 56:151-178.
9. Weil R, Veillette A. Signal Transduction by the Lymphocyte-Specific Tyrosine Protein Kinase p56lck. Current Topics Micro Immunol 1996; 205:63-87.
10. Cushman M, Nagarathnam D, Burg DL, Geahlen RL. Synthesis and Protein-Tyrosine Kinase Inhibitory Activities of Flavonoid Analogues. J Med Chem 1991; 34:798-806.
11. Cushman M, Zhu H, Geahlen RL, Kraker AJ. Synthesis and Biochemical Evaluation of a Series of Aminoflavones as Potential Inhibitors of Protein-Tyrosine Kinases p56lck, EGFr, and p60v-src. J Med Chem 1994; 37:3353-3362.
12. Bylka W, Matlawska I, Pilewski NA. Natural Flavonoids as Antimicrobial Agents. JANA 2004; 7:24-31.
13. Hansch C, Hoekman D, Gao H. Comparative QSAR: Toward a Deeper Understanding of Chemicobiological Interactions. Chem Rev 1996; 96:1045-1076.
14. Afshin F, Razieh S. QSAR Study of p56lck Protein Kinase Inhibitory Activity of Flavonoid Derivatives Using MLR and GA-PLS. Int J Mol Sci 2008; 9:1987-1892.
15. Kramer B, Metz G, Rarey M, Lengauer T. Ligand Docking and Screening with FlexX. Med Chem Res 2009; 9.
16. Cramer III RD, Patterson DE, Bunce JD. Comparative Molecular Field Analysis (CoMFA). 1. Effect of shape binding of steroids to carrier proteins. J Am Chem Soc 1988; 110:5959–5967.
17. Gilbert KM, Skawinski WJ, Misra M, Paris KA, aik NH, Buono RA, et al. Conformational Analysis of Methylphenidate: Comparison of Molecular Orbital and Molecular Mechanics Methods. J Comput Aided Mol Des 2004; 18:719-724.
18. Klebe G, Abraham U, Mietzner T. Molecular Similarity Indices in a Comparative Analysis (CoMSIA) of Drug Molecules to

Correlate and Predict their Biological Activity. J Med Chem 1994; 37: 4130-4146.

19. Cramer III RD, Bunce JD, Patterson DE, Frank IE. Cross validation, Bootstrapping, and Partial Least Squares compared with Multiple Regression Conventional QSAR. Quant Struct-Act Relat 1988; 7:18–25.
20. Kubinyi H. Variable Selection in QSAR Studies. I. An Evolutionary Algorithm. Quant Struct-Act Relat 1994; 13:285-294.
21. Kubinyi H. Variable Selection in QSAR Studies. II. A Highly Efficient Combination of Systematic Seacrh and Evolution. Quant Struct-Act Relat 1994; 13:285-294.